# NONLINEAR DYNAMIC ANALYSIS OF COMPOSITE SANDWICH PLATES WITH DAMPING

K. V. Nagendra Gopal[1], Alok Biswapratap Pani[2]

[1]Department of Aerospace Engineering, Indian Institute of Technology, Madras, Chennai, India-36
Email: gopal@iitm.ac.in
[2]Department of Aerospace Engineering, Indian Institute of Technology, Madras, Chennai, India-36
Email: alokbiswapratap@gmail.com

**Keywords:** Nonlinear vibrations, Viscoelastic, Voigt- Kelvin model, HPM, Struble's technique

**Abstract**
This work presents the geometrically nonlinear free and forced vibration analysis of a simply supported sandwich plate with a soft viscoelastic core. Damping is included by modelling the viscoelastic core as a Voigt-Kelvin solid. The nonlinearity is included in terms of von Karman strains and Reddy's third order shear deformation theory is used to model the deformations. Governing equations are obtained by Lagrange's formulation. A combination of Homotopy perturbation method with Struble's technique is used to solve the strongly nonlinear system for free and forced vibrations for a point load. The variations of nonlinear amplitude and phase difference with forcing frequency are obtained and the influence of layer thickness, length to thickness ratio, applied force and the damping parameter on the damped response is studied.

## 1. Introduction

Sandwich composite panels are widely used in transportation vehicle components and various other applications to achieve high strength to weight ratios. These components are commonly subjected to vibratory motion and also generate undesirable noise. Damping these vibrations and reducing the noise levels is a major goal in the design of these components. Using a soft viscoelastic polymer core in a sandwich construction provides a passive means to control the vibrations. The viscoelastic polymer provides a constrained layer damping (CLD) by inducing high shear strain in the layer upon flexural motion. The difficulty in modeling the response of such structures arises from the geometrical nonlinearity of the large amplitude vibrations and also the frequency dependence of the stiffness. The stress and strain oscillations in viscoelastic materials have a phase difference. This phase difference depends on the amount of damping or the rate of energy dissipation. One commonly used approach is the complex modulus method to account for damping and stiffness. In this work, the viscoelastic behavior of the material is modelled using Voigt-Kelvin spring damper system. The third order shear deformation theory (TSDT) is used to model the plate deflections and the Lagrangian formulation is used to derive the nonlinear equations of motion with Rayleigh's dissipation term. The governing equations are solved using the homotopy perturbation method (HPM), which is more effective and accurate than the traditional perturbation methods in tackling nonlinear problems with very large nonlinearity. The general Struble's technique is combined with HPM to handle the strongly nonlinear differential systems with strong damping effect. The nonlinear response of the system can be examined in terms of the amplitude-frequency and phase-frequency plots. The influence of the geometry, damping and the forcing frequency on the nonlinear response is examined in detail.

## 2. Kinematic formulation and constitutive behavior

### 2.1. Geometrical configuration and material properties

A square sandwich plate with in plane dimension *a* and total thickness *h* as shown in Fig. 1 is considered for the study. The face sheets on top and bottom are cross ply laminates with 0 and 90 degrees orientation for bidirectional strength and the core is a homogeneous isotropic viscoelastic layer for damping. The properties for the core and face sheet materials are given in Table 1.

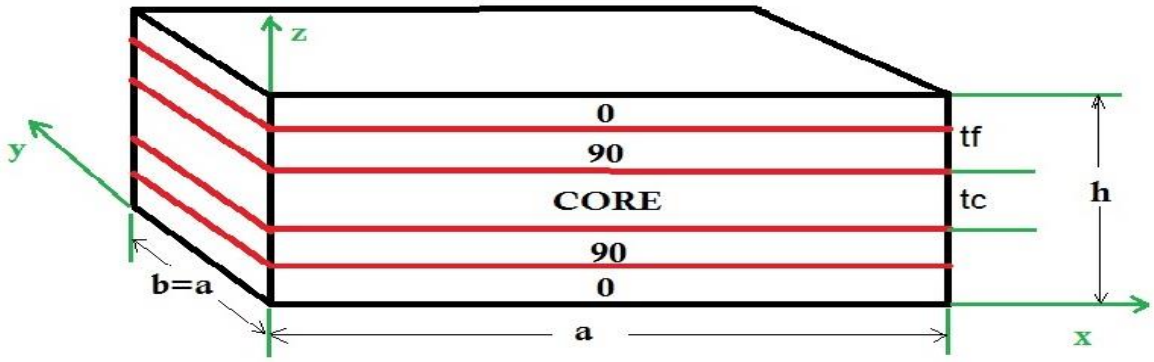


**Figure 1.** Sandwich plate with core and face sheet configuration.

**Table 1.** Material properties

| Face sheet | Core |
|---|---|
| $E_L = 139$ GPa, $E_T = 9.86$ GPa | $E_L = 1.794$ MPa |
| $G_{LT} = G_{TT} = 5.24$ GPa | $\rho = 968.1$ Kg/ $m^3$ |
| $\rho = 1590$ Kg/ $m^3$ | $\nu = 0.3$ |
| $\nu = 0.3$ | |

### 2.2. Kinematic model

The deformations of the plate are assumed according to Reddy's third order shear deformation theory[1]. The displacement fields for the equivalent single layer are cubic functions of z as follows:

$$u = u_0 + z\phi_x + \frac{4z^3}{3h^2}(\phi_x + \frac{\partial w}{\partial x})$$
$$v = v_0 + z\phi_y + \frac{4z^3}{3h^2}(\phi_y + \frac{\partial w}{\partial y})$$
$$w = w_0 \quad (1)$$

The nonlinear strains associated with the displacement fields can be computed using von Karman's reduced nonlinear strain-displacement relations[1], given by:

$$\text{In plane strains}=\begin{Bmatrix} \dfrac{\partial u_0}{\partial x}+\dfrac{1}{2}\left(\dfrac{\partial w_0}{\partial x}\right)^2 \\ \dfrac{\partial v_0}{\partial y}+\dfrac{1}{2}\left(\dfrac{\partial w_0}{\partial y}\right)^2 \\ \dfrac{\partial u_0}{\partial y}+\dfrac{\partial v_0}{\partial x}+\left(\dfrac{\partial w_0}{\partial x}\dfrac{\partial w_0}{\partial y}\right) \end{Bmatrix}+z\begin{Bmatrix} \dfrac{\partial \phi_x}{\partial x} \\ \dfrac{\partial \phi_y}{\partial y} \\ \dfrac{\partial \phi_x}{\partial y}+\dfrac{\partial \phi_y}{\partial x} \end{Bmatrix}-\frac{4z^3}{3h^2}\begin{Bmatrix} \dfrac{\partial \phi_x}{\partial x}+\dfrac{\partial^2 w_0}{\partial x^2} \\ \dfrac{\partial \phi_y}{\partial y}+\dfrac{\partial^2 w_0}{\partial y^2} \\ \dfrac{\partial \phi_x}{\partial y}+\dfrac{\partial \phi_y}{\partial x}+2\dfrac{\partial^2 w_0}{\partial x \partial y} \end{Bmatrix}$$

$$\text{Transverse strains}=\begin{Bmatrix} \gamma_{yz} \\ \gamma_{zx} \end{Bmatrix}=\begin{Bmatrix} \phi_y+\dfrac{\partial w_o}{\partial y} \\ \phi_x+\dfrac{\partial w_0}{\partial x} \end{Bmatrix}-\frac{4}{h^2}\begin{Bmatrix} \phi_y+\dfrac{\partial w_o}{\partial y} \\ \phi_x+\dfrac{\partial w_0}{\partial x} \end{Bmatrix} \tag{2}$$

### 2.3 Voigt-Kelvin model for viscoelastic behaviour

Even though the ultimate concern here is with harmonic motions, the complex moduli approach is not a very convenient way to handle damping in a non-linear system. The method employed here, which is somewhat analogous to the complex moduli approach, is to assume that the core behaves as a Kelvin Voigt solid, whose stress strain relationship is given by:

$$\sigma = E'\varepsilon + E''\dot{\varepsilon} \quad \text{and} \quad \tau = G'\gamma + G''\dot{\gamma} \tag{3}$$

where $\varepsilon$ is a normal strain, $\gamma$ a shear strain, and E", G" are viscoelastic material loss parameters. A relationship between the complex stiffness values and kelvin parameters is desirable. This is readily achieved, as the following discussion shows[2]. Let the complex stiffness values for the isotropic viscoelastic layer are $E = E_1 + iE_2$ and $G = G_1 + iG_2$. It can be established that, for harmonic motion of frequency ω, $E' = E_1$ and $E'' = E_2 / \omega$ and the analogous relations for shear behavior are, $G' = G_1$ and $G'' = G_2 / \omega$.

### 2.4 Constitutive relations

Using the Voigt-Kelvin modelling, the stress strain relationship can be given as:

$$\begin{pmatrix} \sigma_{11} \\ \sigma_{22} \\ \tau_{12} \end{pmatrix}=\frac{E}{1-\gamma^2}\left(\begin{bmatrix} 1 & \nu & 0 \\ \nu & 1 & 0 \\ 0 & 0 & \dfrac{1+\nu}{2} \end{bmatrix}\begin{pmatrix} \varepsilon_{11} \\ \varepsilon_{22} \\ \gamma_{12} \end{pmatrix}+\frac{\xi}{\omega}\begin{bmatrix} 1 & \nu & 0 \\ \nu & 1 & 0 \\ 0 & 0 & \dfrac{1+\nu}{2} \end{bmatrix}\begin{pmatrix} \dot{\varepsilon}_{11} \\ \dot{\varepsilon}_{22} \\ \dot{\gamma}_{12} \end{pmatrix}\right)$$

$$\begin{pmatrix} \tau_{23} \\ \tau_{31} \end{pmatrix}=\begin{bmatrix} G_{23} & 0 \\ 0 & G_{31} \end{bmatrix}\begin{pmatrix} \gamma_{23} \\ \gamma_{31} \end{pmatrix}+\frac{\eta}{\omega}\begin{bmatrix} G_{23} & 0 \\ 0 & G_{31} \end{bmatrix}\begin{pmatrix} \dot{\gamma}_{23} \\ \dot{\gamma}_{31} \end{pmatrix} \tag{4}$$

## 3. Governing equations

The governing equations for the dynamic system are derived as Lagrangian equations of motion including the dissipative terms:

$$(\frac{d}{dt}\frac{\partial}{\partial \dot{q}} - \frac{\partial}{\partial q})(KE - SE) = \frac{\partial WD}{\partial q} + \frac{\partial \tilde{\nu}}{\partial \dot{q}} \tag{5}$$

Where $\tilde{\nu}$ is the Rayleigh's dissipation function.

### 3.1. Boundary conditions

Using Navier's solution[1] approach, the general boundary conditions for a simply supported plate in third order shear deformation theory obtained from a virtual work principle approach are:

$$\begin{aligned}
&u_0\,(x, 0, t)=0,\ \phi_x\,(x, 0, t)=0,\ u_0\,(x, b, t)=0,\ \phi_x\,(x, b, t)=0\\
&v_0\,(0, y, t)=0,\ \phi_y\,(0, y, t)=0,\ v_0\,(a, y, t)=0,\ \phi_y\,(a, y, t)=0\\
&w_0\,(x, 0, t)=0,\ w_0\,(x, b, t)=0,\ w_0\,(0, y, t)=0,\ w_0\,(a, y, t)=0\\
&N_{xx}\,(0, y, t)=0,\ N_{xx}\,(a, y, t)=0,\ N_{yy}\,(x, 0, t)=0,\ N_{yy}\,(x, b, t)=0\\
&\overline{M}_{xx}\,(0, y, t)=0,\ \overline{M}_{xx}\,(a, y, t)=0,\ \overline{M}_{yy}\,(x, 0, t)=0,\ \overline{M}_{yy}\ (x, b, t)=0
\end{aligned} \tag{6}$$

Using the above conditions, the displacements and curvatures can be assumed as a series of harmonic functions.

### 3.2 Lagrangian equations of motion

The final equations of motion obtained after substituting the assumed displacements in the Lagrangian expression and taking the generalized coordinate as U, V, $\theta_x$, $\theta_y$, W respectively

$$\begin{aligned}
&U \Rightarrow 2T_{11}U + T_{12}V + T_{14}\theta_x + T_{15}\theta_y + T_{13}W + T_{132}W^2 = 0\\
&V \Rightarrow T_{12}U + 2T_{22}V + T_{24}\theta_x + T_{25}\theta_y + T_{23}W + T_{232}W^2 = 0\\
&\theta_x \Rightarrow T_{14}U + T_{24}V + 2T_{44}\theta_x + T_{45}\theta_y + T_{34}W + T_{432}W^2 = 0\\
&\theta_y \Rightarrow T_{15}U + T_{25}V + T_{45}\theta_x + 2T_{55}\theta_y + T_{35}W + T_{532}W^2 = 0\\
&W \Rightarrow \frac{I_0 ab}{4}\ddot{W} + D_3\dot{W} + T_{13}U + T_{23}V + T_{34}\theta_x + T_{35}\theta_y + 2T_{33}W + 3T_7W^2 + 4T_8W^3 + 2T_{132}UW\\
&+ 2T_{232}VW + 2T_{432}\theta_x W + 2T_{532}\theta_y W = F_0(t)
\end{aligned} \tag{7}$$

The equations in Eq. 7 are solved to get the *U*, *V*, $\theta_x$ and $\theta_y$ in terms of *W* which gives the final equation to be solved as

$$\ddot{W} + 2\psi\dot{W} + \alpha W + \beta W^2 + \gamma W^3 + \zeta = F_0(t) \tag{8}$$

### 4. Solution

The damped forced vibration problem is solved using HPM with Struble's technique[3], which gives the steady state displacement solution as:

$$W = b\cos(ft + \Omega) + (\frac{\gamma b^3}{16})\frac{(3\psi^2 - 2{\omega_{nl}}^2)\cos 3(qt + \phi) - 3q\psi\sin 3(qt + \phi)}{{\omega_{nl}}^2(3\psi^2 - 4{\omega_{nl}}^2)} \tag{9}$$

The displacement amplitude depends upon the forced frequency by the relations,

$$b(\alpha - \nu^2) + \frac{3\gamma b^3}{4} = F_0\cos\Omega \quad \text{and} \quad 2b\psi\nu = F_0\sin\Omega \tag{10}$$

Eq. 10 gives the backbone curve in the plane (f, b) and the nonlinear phase frequency curve.

## 6. Results and discussion

The effect of nonlinearity can be observed in the magnification plot which bends to one side depending upon the hardening or softening nature of the cubic nonlinearity introduced in terms of higher order strains. For $\omega > \omega_T$, the system has 3 possible values of both amplitude and phase difference. But it chooses one set of values depending upon the sense of change in frequency. Fig. 2 presents the jump phenomenon in amplitude-frequency curve and phase-frequency curve respectively. When the frequency is increased from relatively small value, the amplitude goes on increasing up to point J and the same happens to phase difference in negative direction till it attains –π/2. With a slight increase in frequency after J, amplitude jumps to the lower value possible for the frequency and phase difference jumps to the highest possible value. Similarly, while approaching $\omega/\omega_l = 1$ from a relatively high frequency, the amplitude remains at the lowest value until $\omega_T$ and suddenly jumps to the highest amplitude after that. Phase difference in a similar manner sticks to highest magnitude and jumps to lowest magnitude at $\omega_T$ The intermediate values of amplitude and corresponding phase difference can be regarded as unstable as the system never attains those values.

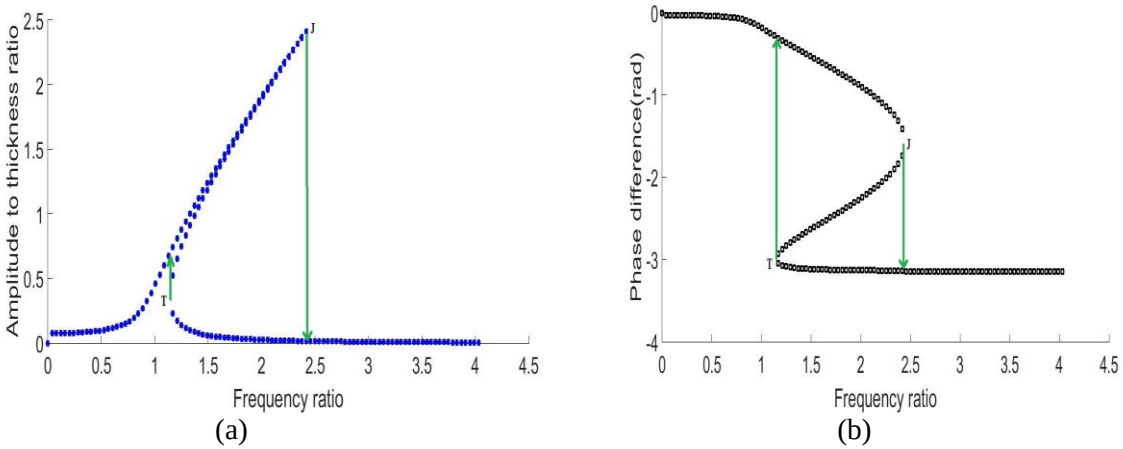


(a) (b)

**Figure 2.** Nonlinear (a)amplitude-frequency and (b)phase frequency plot with jump for a/h=50, $t_c/t_f$ =8, η=0.75, $F_0 = 2000N$

Fig. 3 displays the effect of variation in a/h ratio on the backbone curve. By increasing a/h ratio, the plate approaches the thin plate behavior and it becomes more susceptible to flexural deformation. The coefficients ψ, α and the forcing function $F_0$ are inversely proportional to $(a/h)^2$ and the cubic stiffness γ is inversely proportional to $(a/h)^4$. So with the same load on the plate, the linear stiffness as well as the cubic stiffness are lower for high a/h ratio, thereby resulting in higher displacement amplitudes and straightening of the backbone curve. Due to decrease in nonlinearity, the bulge in phase-frequency curve gets reduced and approaches that of linear system. This effect is accompanied by the decrease in jump frequency at higher a/h ratios.

The effect of the force amplitude for the damped system is shown in Fig. 4. The backbone curves for concentrated force amplitudes 1000N and 2000N at the center of plates with different $t_c/t_f$ and a/h ratios are compared. The results show that by doubling the force amplitude, displacement amplitude for $\omega < \omega_T$ and the lowest amplitude for $\omega > \omega_T$ get nearly doubled for all frequencies but the other two amplitudes for $\omega > \omega_T$ become nearly equal for both force values maintaining the curvature of backbone curve. This indicates that force amplitude has no effect on the nonlinearity of the system, it

only increases the energy of system. The change in phase difference comes in terms of jump condition, which means by increasing the force amplitude, the system attains the jump at a higher frequency.

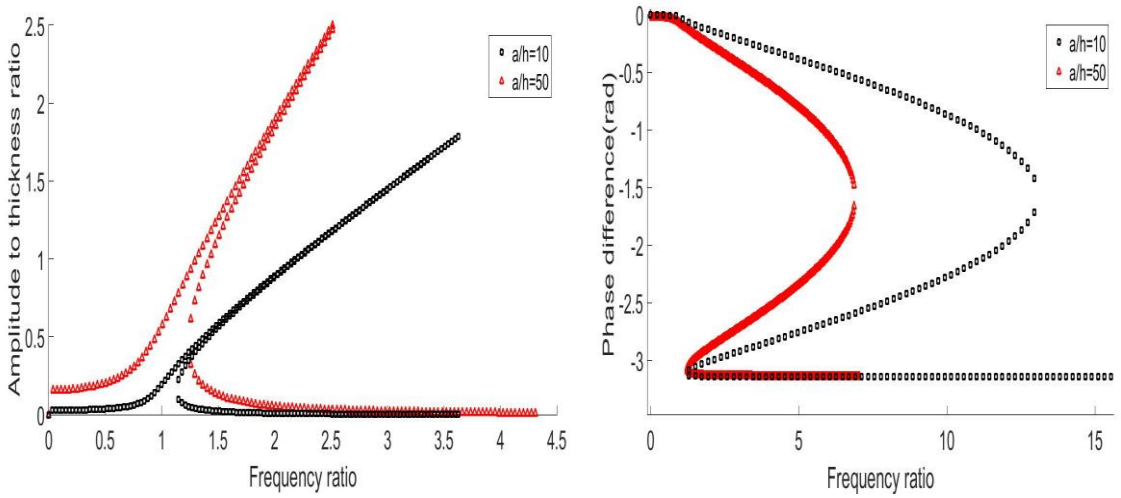


(a) (b)

**Figure 3**. Comparison of nonlinear (a)amplitude-frequency and (b)phase frequency curves for different a/h ratios with $t_c / t_f$ =8, η=0.5, $F_0 = 2000N$

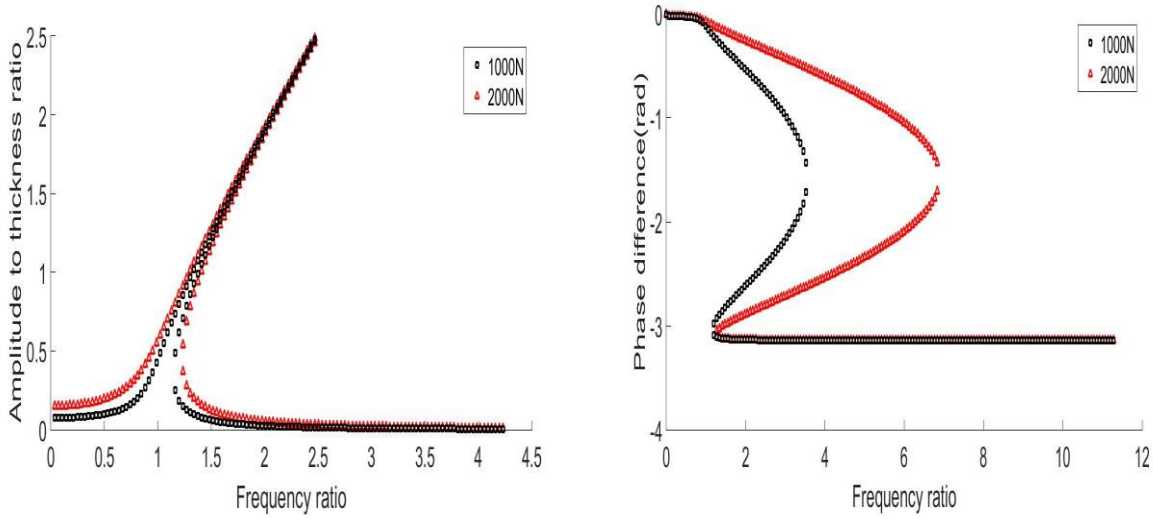


(a) (b)

**Figure 4**. Comparison of nonlinear (a)amplitude-frequency and (b)phase frequency curves for different force amplitudes with a/h=50, $t_c / t_f$ =8, η=0.5

For undamped system, the two arms of amplitude-frequency plot do not intersect each other for any finite frequency. But for damped systems, they intersect which gives the jump frequency. This intersection frequency decreases with increase in damping coefficient of the system. Because the resistance due to damping prevents the system from attaining a higher amplitude value. The bulge in the curve diminishes with increase in viscosity parameter(η). This is because by increasing the damping on the system, the maximum amplitude attainable at the jump point(J) decreases and the jump occurs at an earlier frequency. The effect of viscosity parameter on amplitude and phase difference is given in Fig. 5.

For *a* and *h* values individually taken constant, the amplitude corresponding to any frequency increases with increase in $t_c / t_f$ ratio. This is obvious because by increasing the proportion of core the overall stiffness of the plate gets reduced thereby allowing more deformation. But the important thing to notice is the effect on nonlinearity or the cubic stiffness. For *a*/*h*=10 i.e. in the range of thick plates, nonlinearity increases with increase in core proportion as seen in Fig. 6(a). But the opposite happens for thin plates like *a*/*h*=50 which is given in Fig. 7(a).

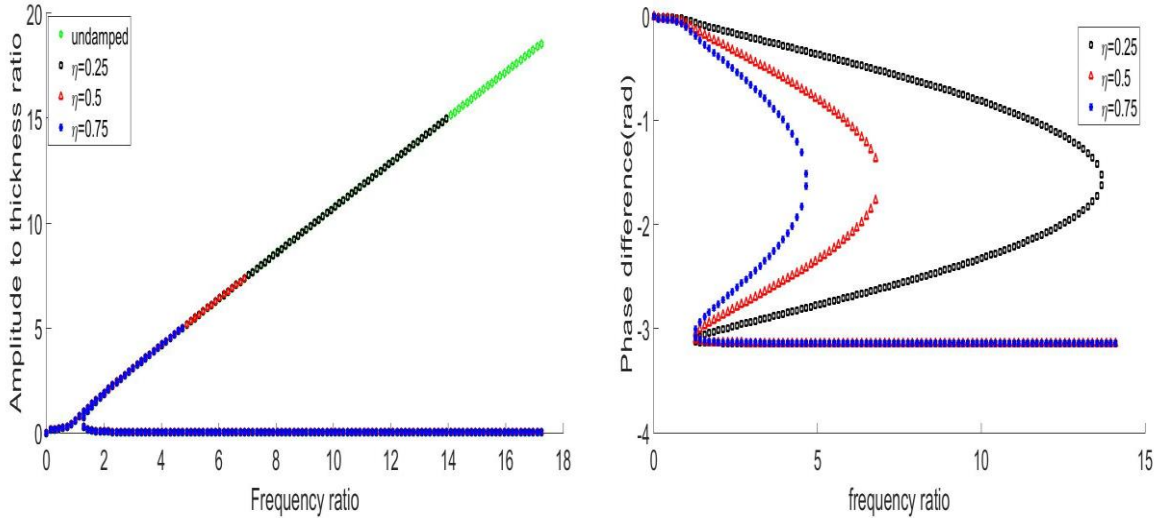


(a) (b)

**Figure 5**. Comparison of nonlinear (a)amplitude-frequency and (b)phase frequency curves for different damping parameters with a/h=50, $t_c / t_f$ =8, $F_0 = 2000N$

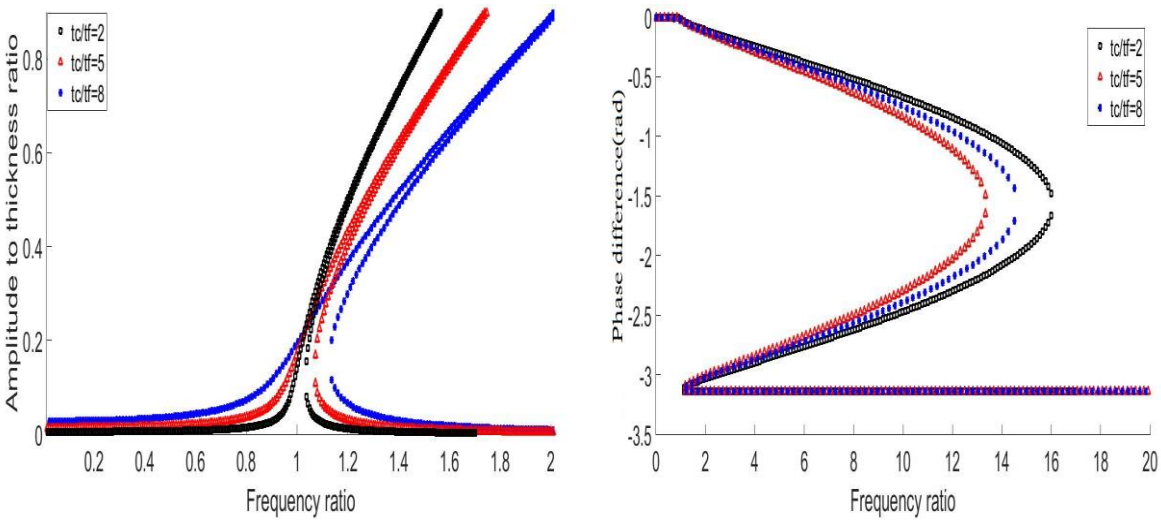


(a) (b)

**Figure 6**. Comparison of nonlinear (a)amplitude-frequency and (b)phase frequency curves for different $t_c / t_f$ ratios with a/h=10, η=0.5, $F_0 = 2000N$

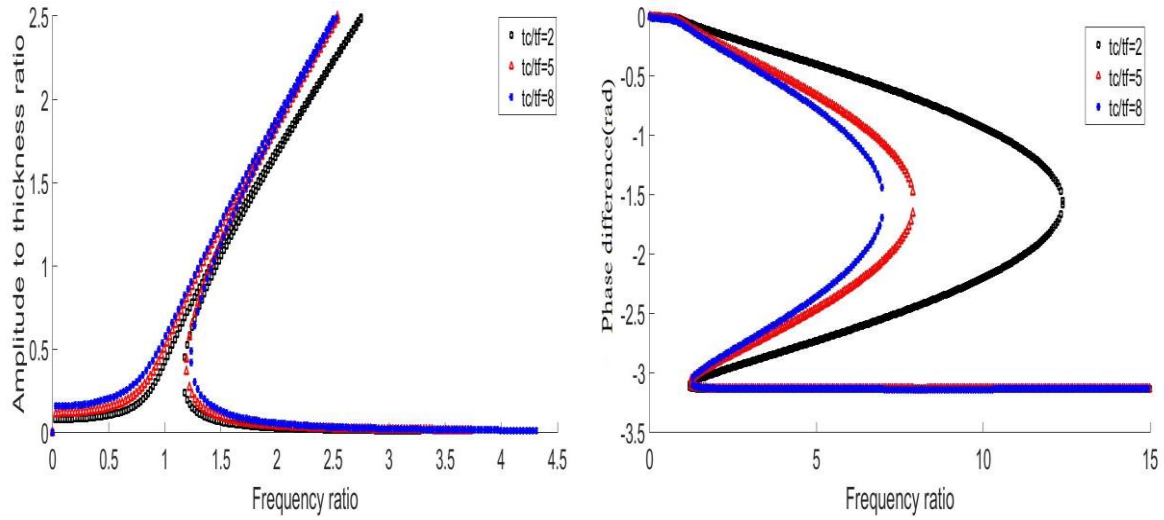


(a) (b)

**Figure 7**. Comparison of nonlinear (a)amplitude-frequency and (b)phase frequency curves for different $t_c / t_f$ ratios with a/h=50, η=0.5, $F_0 = 2000N$

The behavior of phase frequency curve under variation in $t_c / t_f$ ratio which is entirely dependent upon the jump frequency is presented in Fig. 5(b) and 6(b). For $\omega < \omega_T$ the phase values follow the same pattern as amplitudes having a higher value for higher $t_c / t_f$ ratio with constant plate thickness. But for $\omega > \omega_T$, the bulges take their respective positions depending upon the jump frequency.

## 7. Conclusion

In this paper, only the first mode of vibration with m,n=1 of the simply supported plate is considered for simplicity of the solution process. The Voigt-kelvin spring damper model is used to model the viscoelastic behavior of the core and the stiffness and damping parameters in the model are obtained by developing a relationship with the complex moduli of the viscoelastic material. This kind of modeling can be used to produce an analysis similar to single dof systems as it effectively reduces the coupled set of governing equations into a single nonlinear differential equation. The problem is solved using HPM with struble's technique, which is very effective for nonlinear damped systems and also gives same results as simple HPM with zero damping. This method only gives the solution to the steady state response, so cannot be used for free damped vibration problems. The accuracy of the solution can be improved by including the neglected terms and solving the coupled set of equations simultaneously. A matrix solution method with HPM can be approached for solving similar problems with complex boundary conditions or different layer arrangements.

## References

[1] Junuthula Narasimha Reddy. Mechanics of laminated composite plates and shells: theory and analysis. CRC press, 2004.
[2] EJ Kovac Jr, William J Anderson, and RA Scott. Forced non-linear vibrations of a damped sandwich beam. Journal of Sound and Vibration, 17(1):25-39, 1971.
[3] Md Abdur Razzak and Md Helal Uddin Molla. A new analytical technique for strongly nonlinear damped forced systems. Ain Shams Engineering Journal, 6(4):1225-1232, 2015.